

# Top-Related Meta-Learning Method for Few-Shot Detection

Qian Li \*

State Key Laboratory of Computer Architecture, Institute of Computing Technology,  
University of Chinese Academy of Sciences, Beijing, China  
liqian18s@ict.ac.cn

Nan Guo

State Key Laboratory of Computer Architecture, Institute of Computing Technology, Beijing, China  
guonan@ict.ac.cn

Xiaochun Ye, Duo Wang, Dongrui Fan and Zhimin Tang

State Key Laboratory of Computer Architecture, Institute of Computing Technology,  
University of Chinese Academy of Sciences, Beijing, China  
{yexiaochun, wangduo18z, fandr, tang}@ict.ac.cn

## Abstract

Many meta-learning methods are proposed for few-shot detection. However, previous most methods have two main problems, poor detection APs, and strong bias because of imbalance datasets. Previous works mainly alleviate these issues by additional datasets, multi-relation attention mechanisms and sub-modules. However, they require more cost. In this work, for meta-learning, we find that the main challenges focus on related or irrelevant semantic features between different categories, and poor distribution of category-based meta-features. Therefore, we propose a Top-C classification loss (i.e. TCL-C) for classification task and a category-based grouping mechanism. The TCL exploits true-label and the most similar class to improve detection performance on few-shot classes. According to appearance and environment, the category-based grouping mechanism groups categories into different groupings to make similar semantic features more compact for different categories, alleviating the strong bias problem and further improving detection APs. The whole training consists of the base model and the fine-tuning phase. During training detection model, the category-related meta-features are regarded as the weights to convolve dynamically, exploiting the meta-features with a shared distribution between categories within a group to improve the detection performance. According to grouping mechanism, we group the meta-features vectors, so that the distribution difference between groups is obvious, and the one within each group is less. Extensive experiments on Pascal VOC dataset demonstrate that ours which combines the TCL with category-

based grouping significantly outperforms previous state-of-the-art methods for few-shot detection. Compared with previous competitive baseline, ours improves detection AP by almost 4% for few-shot detection.

## 1. Introduction

Recently, neural network has progressed quickly for computer vision. Various efficient methods [32] [33] [42] [21] depend on large labeled datasets. However, when datasets are insufficient, it may result in overfitting and hurting generalization performance. On the contrary, there is a quite difference between the human vision system and the computer vision system. For the unlabeled datasets, the human vision system can classify, locate and describe. Computer systems cannot do those. Despite state-of-the-art most methods may succeed, they require more expensive datasets that are the labeled with auxiliary descriptions, such as shape, scene or color etc.

The predecessors propose few-shot learning methods [16] [6] [39], solving the above issues, and few-shot learning includes classification, detection and segmentation. Few-shot detection [8] [31] [37] is one of the most challenging tasks. This paper finds two main challenges. First, due to just few samples, the features which are extracted from standard CNNs are not suitable for few-shot learning, directly. In previous most state-of-the-art few-shot learning methods, the classification is often regarded as the standard task. For each iteration of training, classification is a binary classification task for YOLOv2 [33], resulting in bias problem and hurting performance on the other classes. Then, many methods [30] [46] [18] are proposed for auxiliary fea-

\*<https://github.com/futureisatyourhand>

tures related to description. However, it is difficult to ensure whether the external datasets are beneficial and tell which is noise. Therefore, many methods [30] [47] [46] learn auxiliary features by sub-modules to improve performance, requiring more labeled datasets and more parameters.

In order to solve those problems, based on [19], we propose a new top classification loss (i.e. TCL) for few-shot learning to improve performance of few-shot detection. For YOLOv2 [33] classification is a binary classification task and ignores other results. Although the Cross-Entropy loss [35] or Focal loss [25] can reduce the trust on the original label and increase the trust on the other labels to a certain extent. That cannot ensure that other categories-based features except for the true label are bad for learning features, hurting detection performance because of few samples. Many researchers exploit the label smoothing and Cross-Entropy to alleviate the problem. However, they do not eliminate category-based irrelevant features and enhance the learning of similarity semantic features for different categories. Smoothing label may increase irrelevant semantic features of other classes and hurt performance for few-shot learning. Therefore, except for the true-label prediction, for the most similar prediction, no matter help or hurt few-shot detection, we can solve this problem by setting only a simple constraint. In this paper, for every sample, except for the true-label, we only constrain the false result which is most likely to be predicted as true class, enhancing the semantic features relating with the true-label and suppressing irrelevant semantic information.

Then, without additional datasets, we propose a category-based grouping mechanism only by labels. As shown in Figure 1 (a), the left in the first row is the object "aero" and the last one in the same row is "bird", they are similar in appearance. In most conditions, they often exist on the same environment. Every two stacked samples belong to a class, these are also very similar in appearance. And the scenes are also similar between objects in 1th, 2th, and 4th column, and between objects in 3th and 5th column. As seen in Figure 1, we split all classes into disjoint groups. Therefore, this work proposes a category-based grouping mechanism to assist model learn meta-features better. Very few methods without additional datasets have found the characteristic, applying that into few-shot detection. Without additional parameters and datasets, we alleviate the strong bias problem between all classes and further improve few-shot detection APs by the category-based grouping. For few-shot detection, our contributions are as follows:

- We design a top classification loss (TCL), which allows the true-label and the false label which is most likely to be predicted as true label to improve performance of few-shot detection, together.
- Based on categories, we find the similar appearance and the scene between different categories. We group all classes into sub-groups with disjoint each other. Then, we construct a category-based grouping loss on meta-features, which alleviates the strong bias problem and further improves detection APs of few-shot.
- We experiment different classification losses for few-shot detection on Pascal VOC, and all results show that our TCL performs better.
- Combining the TCL with category-based grouping mechanism, for  $k$ -shot detection,  $k = 1, 2, 3$ , the detection APs achieve almost 20%, 25%, 30%, respectively. Experimental results show that ours outperforms the state-of-the-art, and grouping is beneficial for concentration of detection APs between all classes.

## 2. Related Work

This paper focuses on few-shot learning. Based on the meta-learning, [14] [11] and [17] regard classes with only few samples as novel classes. Our work studies the classification loss, meta-learning methods, and detection for few-shot learning.

**Classification Loss.** Different classification losses, such as the BCEwithLogits, the Cross-Entropy loss with SoftMax[35] [27] [26], are proposed. Most computer vision tasks use the Cross-Entropy to implement training. Then, [25] proposes a focal loss to alleviate the imbalance between the positive and negative samples. However, many tasks based on YOLOv2 [33] just exploit a binary classification loss, resulting in the imbalance and ignoring the correlation about categories. In this paper, for few-shot classes, we assume that too much noise can hurt the detection performance, and only the true-label may fail in learning relation with other categories. Therefore, we propose the TCL for classification task, which only focuses on the true-label and the most similar class. Compared with [4] which increases the distance between classes, our TCL only exploits semantic information to promote performance.

**Meta-Learning.** In recent years, different meta-learning algorithms have been proposed, including metric-based [23] [45] [24] [20], memory networks [38] [29] [1], and optimization [15] [22] [13] [12]. The first type learns a metric based on few samples given and score a label of the target image according to similarity. The second is cross-task learning, and most memory networks widely are model-independent adaptation [12]. A model is learned on a variety of different tasks, making it possible to solve some new



(a) The visualization of category grouping.

group	Class					
1	aero	bird				
2	cow	horse	cat	sheep	dog	
3	sofa	chair				
4	tv	plant	table			
5	boat	bicycle	train	car	bus	mbike
6	bottle	person				

(b) Category-based grouping table on Pascal VOC dataset.

Figure 1. Overall scheme of category-based grouping mechanism. In (a), all categories are divided into  $K$  groups. All categories in each row are similar in appearance and environment appeared. All categories in each row are a group. When “bird” is flying, it looks like “aero”. “cows, horses, cats, sheep and dogs” have four legs and similar shape, and they often appear in similar environments. We regard them as a group. In this work, we experiment Pascal VOC dataset. As detailed in (b), all categories of Pascal VOC dataset are divided into 6 (i.e.  $K=6$ ) groups by (a). The appearance and the appeared environment are very similar for different categories within a group.

learning tasks with only few samples. Many researchers propose many variants [28, 41] [2] [36]. The last one is a parameter prediction. Corresponding to an image of each category for every iteration, the category-based meta-features are regarded as the weight, learning the parameters of the network layer dynamically. In inference, it is not necessary to train to adapt the learned features of each category to the new category. Most works apply this method to the classification task. [19] detects objects by Yolov2 [33], and based on that, we further improve performance and alleviate many problems for few-shot detection.

**Few-shot Detection.** Previous most detection methods focus on limited labeled datasets. The weakly-supervised methods [5] [43] [40] only consider detectors on image-level labels. Some works [18] [44] [9] only use few samples with bounding box level annotations for each class, and generate pseudo labels on many images to detect objects. Many zero-shot methods [3] [31] use sub-module to detect. [7] transfers the basis domain to the novel. [10] based on [34] exploits attention-RPN and three relations to improve performance of few-shot detection, and increases more parameters and makes training slower. Therefore, we only split all categories into disjoint groups to improve detection performance without additional sub-modules, and captures the correlation between groups or categories from the category-based meta-features. from the category-based meta-features.

### 3. Our Approach

As shown in Figure 2, we propose the TCL for classification and category-based grouping mechanism to help meta-learning model [19] learn the related features between categories. The input of the meta-model  $M$  is an image and a mask of only an object selected randomly. The value of the mask within object is 1, otherwise, it is 0. The number of the meta-model input is divisible by the number of all categories about training. For the Pascal VOC dataset,

when training the base model, the inputs of the meta-model are  $15n$  samples, while fine-tuning, which are  $20n$  samples,  $n$  is the number of GPUs. The meta-model extracts meta-feature vectors about classes as the weight for dynamic convolution, then, the classifier and detector complete classification and regression task. During training, we use the TCL to training classification. According to category grouping mechanism, we split category-based meta-feature vectors into groups to learning better meta-features.

#### 3.1. Feature Reweighting for Detection

Different categories may have a common and unique distribution. As shown in Figure 2, based on YOLOv2 [33], this method uses a meta-model  $M$  to obtain meta-feature about categories as dynamic weights for dynamic convolution. The meta-learning model takes each annotated sample  $(I_i, B_i)$ , and for the category  $i$ ,  $i = 1, 2, \dots, N$ ,  $N$  represents the number of categories.  $I_i$  and  $B_i$  represent the reference image and the selected mask of only an object on  $i$ th class, obtaining category-based meta-feature by  $M$ . The  $M$  learns to predict  $N$  sets of correlation coefficients  $W$ ,  $W = \{w_1, w_2, w_3, \dots, w_N\}$ , where  $w_i$  represents the dynamic weight of the  $i$ -th category,  $w_i = M(I_i, B_i)$ ,  $M$  is the meta-model. Based on Darknet-19, the author builds a feature extractor  $D$  which extracts basis features  $F_j$  from the image  $S_j$ :  $F_j = D(S_j)$ . Then, for class  $i$ , the weighted feature vector is obtained according to  $w_i$  and  $F_j$ :  $F_{j,i} = F_j \otimes w_i$ . This approach can adapt the features to the novel classes. Finally, based on  $F_{j,i}$ , the author uses classifier and detector to classify and regress. See [19] for details

#### 3.2. TCL-C

For few-shot detection, especially for meta-learning, we use the TCL-2 to encourage model to train classification by the true-label and the false result which is most likely to be predicted as true result, enhancing the semantic features

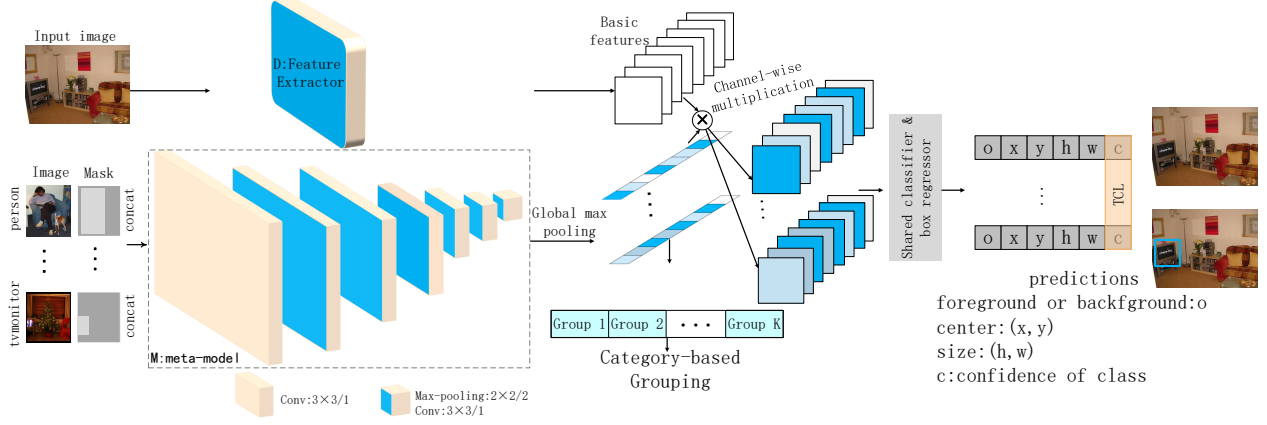


Figure 2. Overall structure of our method. The detection model consists of a feature extractor  $D$  and a meta-model  $M$ .

relating with the true-label and suppressing irrelevant semantic information. The TCL makes the features tend to learn the true-label and controls effect of the most similar label by  $\beta^+$  and  $\beta^-$ , respectively, improving performance on novel (i.e. few-shot) classes. Therefore,  $\beta^+$ ,  $\beta^-$  denote the two expectations, the classification score of true-label, and highest classification score except for the true-label, respectively.  $\eta$  and  $\gamma$  affect the convergence rate. Detailed in Equation 1 below.

$$\begin{aligned} L_{cls} &= L_{cls}^{pos} + L_{cls}^{neg} \\ L_{cls}^{pos} &= \log(\eta + e^{\gamma(\beta^+ - P_t)}) \\ L_{cls}^{neg} &= \log(\eta + e^{\gamma(F_t - \beta^-)}) \end{aligned} \quad (1)$$

where  $L_{cls}^{pos}$  and  $L_{cls}^{neg}$  represent the loss functions for the true-label class and the most similar class, respectively. They weaken the effect from other classes.  $P_t$  and  $F_t$  represent the prediction on the true-label class, and the prediction of the most similar class, respectively. When classification score of the true-label class is the highest,  $P_t$  is expected to be close to  $\beta^+$ , at this time, we expect the  $F_t$  (the prediction with the second highest score by category) to be close to  $\beta^-$ . Otherwise, we expect the  $F_t$  (i.e. the highest classification score) to be close to  $\beta^-$ . By the mechanism, we urge the model to distinguish between the semantic features of the two most similar categories, improving the detection APs on few-shot(novel) classes.

During analysis, as detailed in Equation 1, we only experiment TCL-2. When  $C$  is bigger than 2 for TCL-C, how much influence other classes except for the true-label have on detection, we need to adjust the threshold value of each category dynamically to apply to the true-label, which requires extensive experiments. Otherwise, theoretically, TCL-C and the label smoothing are quite similar. Then, there is no guarantee how much categories-based features of other classes except for the true label are beneficial for

classification, and we will experiment it in the future. Detail as follows,  $0 \leq \beta_k^- \leq 1$ ,  $\beta_k^-$  is the expected threshold for the  $k$ th (i.e.  $k=1, 2, \dots, C$ ) similar category.

$$\begin{aligned} L_{cls}^{neg} &= \log(\eta + e^{\gamma(F_t^1 - \beta_1^-)}) + \log(\eta + e^{\gamma(F_t^2 - \beta_2^-)}) \\ &\quad + \dots + \log(\eta + e^{\gamma(F_t^k - \beta_k^-)}) + \dots + \\ &\quad \log(\eta + e^{\gamma(F_t^C - \beta_C^-)}), 2 \leq C < N \end{aligned} \quad (2)$$

### 3.3. Category-Based Grouping

As detailed in Figure 2, meta-learning uses the correlation between categories for few-shot detection. As shown in Figure 1, without additional datasets, our grouping mechanism focuses on appearance, followed by the environment, splitting all categories into groups which are disjoint with each other. We mainly analyze the mean and variance of the category-based meta-feature distribution from  $M$ . As for the principle (see Figure 1), as shown in Equation 3, the intra-group distance is smaller and the inter-group distance is larger. The paper divides the 20 classes of Pascal VOC DataSet into 6 groups, and proposes a category-related loss about groups. Our method encourages the variance of the mean value of the feature vector smaller for every group, making the semantic feature distribution more compact between categories within each group, and helps the feature distribution sparser between groups, improving detection APs and reducing the detection dispersion on the all categories.

As detailed in Equation 3(next page), where  $W_{mean-std}^j$  represents the distribution dispersion of the mean value of the meta-feature space between categories in group  $j$ , and we expect it to be as small as possible.  $W_{std}^j$  represents the dispersion metric of the variance of the feature distributions in group  $j$ ,  $W_{mean}^j$  represents the mean metric of the mean of the feature distributions in the group  $j$ , and we quantify the dispersion



$$L_{re-meta} = \sum_{j=1}^K \log\left(\tau + \frac{W_{mean-std}^j}{\epsilon + \frac{1}{W_{mean-std}^j} + \sum_{k=j+1}^K (e^{(W_{std}^j - W_{std}^k)^2} + e^{(W_{mean}^j - W_{mean}^k)^2})}\right) \quad (3)$$

and concentration of the two distributions, respectively. According to Equation 3, we expect the distribution of different categories within the groups is more compact, and the different groups are farther from each other.  $W_{mean-std}^j$  is smaller, then,  $W_{std}^j - W_{std}^k$  and  $W_{mean}^j - W_{mean}^k$  are bigger. Every theory is detailed below.

$$W_{mean-std}^j = \sqrt{\frac{1}{C_j} \sum_{m=1}^{C_j} (u_m^j - u^j)^2} \quad (4)$$

where we expect the value to be smaller.  $u^j$  is the mean of all features for the  $j$ th group.  $C_j$  represents the number of categories belonging to the group  $j$ th.

$$W_{std}^j = \begin{cases} \sqrt{\frac{1}{C_j} \sum_{m=1}^{C_j} (\delta_m^j - \delta^j)^2}, & C_j > 1. \\ \delta_m^j, & C_j = 1. \end{cases} \quad (5)$$

where  $W_{std}^j$  represents the space of dispersion about all category-based meta-features vectors for  $j$ th grouping. According to Equation 3, We expect the distance is more obvious between groups and smaller within a group. When there is more than one category in group  $j$ ,  $W_{std}^j$  obtains the dispersion between categories within  $j$  group.

$$W_{mean}^j = \begin{cases} \frac{1}{C_j} \sum_{m=1}^{C_j} u_m^j, & C_j > 1. \\ \delta_m^j, & C_j = 1. \end{cases} \quad (6)$$

where  $W_{mean}^j$  obtains the mean metric of meta-features distribution for all categories of the  $j$  group. Otherwise, it only explains the dispersion corresponding to the category.

$$u_i = \frac{1}{|F|} \sum_{f=1}^{|F|} x_f^i, \quad \delta_i = \sqrt{\frac{1}{|F|} \sum_{f=1}^{|F|} (x_f^i - \bar{x}^i)^2} \quad (7)$$

where  $x$  denotes that the category-related  $|F|$ -dimension meta-feature vectors,  $|F| = 1024$ ,  $i = 1, 2, 3, \dots, N$ . As shown in Figure 1, all 20 categories are divided into 6 groups,  $K = 6$ ,  $C_j \subset \{C_1, C_2, \dots, C_6\}$ , and  $C_j$  represents the number of categories in  $j$  group,  $j = 1, 2, \dots, 6$ . Because of the correlation loss of each group, the value of the  $\log$  function is less than 0. Therefore, the parameter  $\tau$  is

used to ensure that the loss is a positive value, and the parameter must be greater than or equal to 1. In terms, the method alleviates the phenomenon which the performance on different categories varies greatly for few-shot detection.

### 3.4. Loss Details

**Category-Based Grouping.** Considering that different categories in different environments have the similar appearance and different categories are in the similar environment, in order to reduce the setting, we mainly focus on the appearance similarity, followed by the environment, and we set objects with the similar appearance and scenes appeared as a group. As shown in Figure 1 (b), we divide the Pascal VOC with 20 categories into 6 groups, namely  $K = 6$ . As shown in the Equation 3, we set the parameter  $\tau$ ,  $\epsilon$  to 1 and 0.00005 respectively.

**Loss Functions.** In order to train the meta-model and ensure that the shared features (i.e. within a group) are more compact between the meta-features of the similar semantic objects, we jointly train classification, category-based grouping, and regression, as shown in Equation 8. Compared with state-of-the-art classification methods, our TCL-2 method is more suitable for few-shot detection.

$$L_{loc} = L_{loc}(x) + L_{loc}(y) + L_{loc}(w) + L_{loc}(h) \quad (8)$$

$$L = \alpha L_{cls} + \omega L_{re-meta} + \lambda L_{loc}$$

where  $L_{re-meta}$  denotes the category-based grouping loss.  $L_{loc}$  includes the center location loss  $L_{loc}(x)$ ,  $L_{loc}(y)$  and scale loss  $L_{loc}(w)$ ,  $L_{loc}(h)$ . In this experiment, the classification, similarity, and regression balance parameters,  $\alpha$ ,  $\omega$  and  $\lambda$ , are set to 1, 6, and 1, respectively.

## 4. Experiments and Results

This experiment consists of the base training and few-shot fine-tuning. As shown in Figure 2, the output of the meta-model  $M$  is related to the number of categories, and each category-based meta-feature vector is represented as a 1024-dimension vector. We experiment with different classification losses, BCEwithLogits, Focal [25], Cross-Entropy [35] and the TCL-2, combining with the Category-based Grouping, respectively. Methods which combine all classification losses and our proposed category-based grouping are regarded as Re-BCEwithLogits, Re-Focal, Re-Cross-Entropy, and Ours, respectively. Detail as follows.

#### 4.1. DataSets and Setting

The Pascal VOC DataSet contains 20 categories, we randomly select 5 categories as novel(i.e. few-shot) categories for fine-tuning, and the remaining 15 categories as base classes for the base model. The 20 categories are randomly divided into 6 novel parts, and we experiment 3 parts obtained as the novel classes for fine-tuning  $k$ -shot,  $k = 1, 2, 3, 5$ . Our setting is the same with [19]. During base classes training, only samples with 15 categories are trained, and the remaining regarded as novel classes with 5 categories are fine-tuned, and each novel class has only  $k$ -shot, named 5-way  $k$ -shot. For meta-model, when there are multiple objects in an image, only an object mask is randomly selected corresponding to the classes. All models are trained by 4 GPUs with 64 batch sizes, and we train for 80,000 iterations for base model. In our work, we use test sets of VOC2007 as our test sets, and training/validation sets of VOC2007 and VOC2012 as our training sets. We use SGD with momentum 0.9, and L2 weight-decay 0.0005 for detector and meta-model.

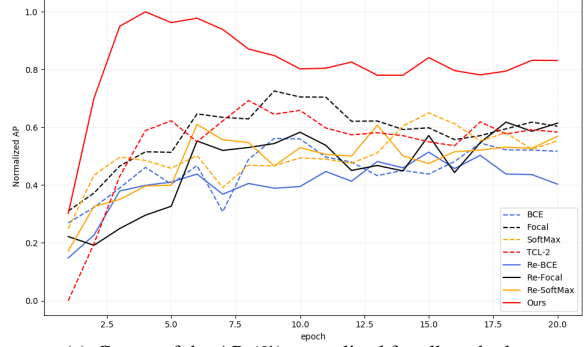
#### 4.2. Ablation Studies

Our experiments are mainly for 5-way  $k$ -shot. We analyze the detection performance for the Pascal VOC by the category-based meta-feature grouping loss and different classification losses. The details are as follows.

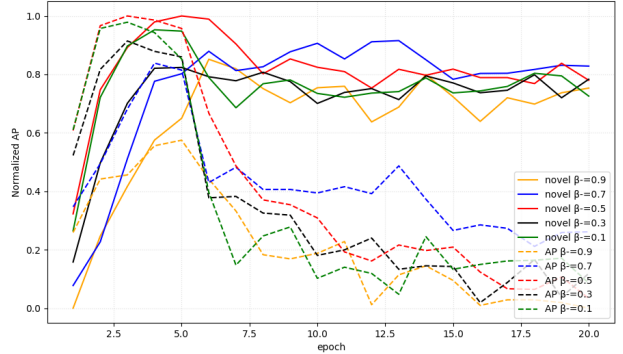
##### 4.2.1 The Importance of the TCL

**Impact of  $\beta^-$ .** As shown in Equation 1,  $\beta^-$  is essential for our TCL-2. The threshold of true label  $\beta^+$  is 1.0, the negative with the highest score denotes the threshold  $\beta^-$ , and we set to 0.5.  $\beta^-$  cannot be too large or small. If it is too large, making meta-model drive the other samples towards the true-label. Otherwise, it makes the model trust only the true-label, and violates the principle of similarity and reduces performance on few-shot(i.e. novel) classes. As illustrated in Figure 3(b), when the  $\beta^-$  is greater than 0.5, the APs distribution on the novel classes(see the solid line) is consistent, and best APs on all categories(see the dashed line) is lower than our setting,  $\beta^- = 0.5$ . When  $\beta^-$  is less than 0.5, the APs on the novel classes tend to be smooth because the semantics between the true-label and the most similar sample are clearly separated to the maximum, making model trust the true-label most and failing to weaken the assistance of false true result. Therefore, when the  $\beta^-$  is set to 0.5, our method can exploit similar semantics distribution between different categories to improve the performance on novel classes better.

**Comparison with the state-of-the-art losses.** As shown in Table 1, compared with the state-of-the-art BCE-withLogits, Focal [25], and Cross-Entropy [35], our TCL-2 can improve the few-shot detection performance. For novel



(a) Curves of the APs(%) normalized for all methods.



(b) Curves of the APs(%) normalized for different  $\beta^-$ .

Figure 3. For Pascal VOC, in (a), for novel set1 2-shot, the curve shows all epochs fine-tuning results of the detection APs (%) on the novel classes. Our method obviously outperforms others. In (b), Results with solid line are normalized AP on the novel classes, and results with the dashed line are the detection normalized AP on all categories. For TCL-2 loss, when the  $\beta^-$  is set to 0.5, our method is better for fine-tuning novel1 2-shot.

set 1, the 1-shot detection APs of TCL-2 is 2.73%, 2.88%, and 3.78% better than the other classification losses, respectively. The TCL-2 is better than the other classification methods by 1.23%, 0.73%, and 5.53% for 3-shot, respectively. On the other hand, as seen in Figure 3(a), compared with all classification losses, the TCL-2 can balance the detection APs on all categories better. As shown in Table 2, for novel set1, our TCL-2 can alleviate the strong bias problem. Especially for 1-shot detection dispersion on all categories, the TCL-2 is 2.04%, 4.0%, and 4.15% lower than the BCE-withLogits, Focal and Cross-Entropy, respectively.

##### 4.2.2 Analysis of the Category-based Grouping

**Impact on every strategy.** We design the scheme in Equation 9 by category-based grouping mechanism (i.e. Figure 1). Then, the experiment analyzes every component (i.e.

	Novel Set1				Novel Set2				Novel Set3			
Method/shot	1	2	3	5	1	2	3	5	1	2	3	5
BCEwithLogits	16.42	18.51	27.41	36.07	13.59	14.71	26.3	35.2	15.1	15.62	26.14	31.6
Re-BCEwithLogits	13.26	17.46	24.31	33.76	<b>18.29</b>	19.71	26.99	35.3	11.0	13.0	20.74	31.95
Focal	16.27	21.63	27.91	<b>37.43</b>	10.39	15.23	18.36	34.09	9.6	8.87	20.16	27.54
Re-Focal	18.22	20.05	20.45	36.15	14.16	15.88	23.13	27.2	7.3	8.67	16.35	28.6
Cross-Entropy	15.37	19.11	23.11	35.18	16.04	19.2	25.46	35.84	12.19	15.3	20.31	31.91
Re-Cross-Entropy	18.55	21.02	22.25	36.5	15.15	20.81	26.07	33.45	13.07	14.53	23.93	35.58
TCL-2	19.15	21.23	28.64	36.94	17.56	22.25	25.57	38.45	12.27	17.33	<b>30.81</b>	35.08
Ours	<b>20.08</b>	<b>26.75</b>	<b>29.76</b>	36.28	18.07	<b>24.66</b>	<b>30.94</b>	<b>39.04</b>	<b>19.42</b>	<b>17.43</b>	23.24	<b>37.66</b>

Table 1. The results of detection APs(%) on novel classes. For few-shot detection on Pascal VOC, our method significantly outperforms others.

Shot/Method	BCEwithLogits	Re-BCEwithLogit	Focal	Re-Focal	Cross-Entropy	Re-Cross-Entropy	TCL-2	Ours
1	55.04	58.58	57.0	54.77	57.15	53.86	53.0	<b>52.63</b>
2	52.84	54.46	57.0	51.99	53.36	50.63	50.93	<b>46.45</b>
3	45.81	48.28	45.67	51.22	49.63	48.6	45.46	<b>44.37</b>
5	41.1	42.07	<b>40.74</b>	32.57	41.95	40.64	41.82	41.36

Table 2. Dispersion of the detection APs(%) on all categories. For novel set1, our method obviously alleviates the strong bias, reducing dispersion of detection performance.

$q_j, Q_j$  and  $U_j$ ).

$$L_{re-meta} = \sum_{j=1}^K \log\left(\tau + \frac{q_j}{\epsilon + Q_j + \sum_{k=j+1}^K U_j}\right). \quad (9)$$

Except for the best strategy (Equation 3), we experiment three other strategies, details as follows:

$$q_j = 1, Q_j = 0, U_j = e^{(W_{std}^j - W_{std}^k)^2} \quad (10)$$

where related grouping is only related to meta-feature distribution between groups, the method fails to learn the mean distribution of all meta-feature vectors between groups. Therefore, we optimize the component  $U_j$ , as detailed below:

$$q_j = 1, Q_j = 0 \\ U_j = e^{(W_{std}^j - W_{std}^k)^2} + e^{(W_{mean}^j - W_{mean}^k)^2} \quad (11)$$

$U_j$  can learn features between groups. However, the method cannot success in learning meta-feature distribute within a group. Then, our final category-based grouping (Equation 3) makes the distribution of meta-features more compact within a group and the difference between groups more obvious.

In the other hand, if the category-based grouping is only attribute to the disperse of meta-feature between groups and similarity between categories within a group, grouping mechanism cannot learn the difference of mean metric of meta-features between groups, resulting in lower mean

APs, detail as follow:

$$q_j = W_{mean-std}^j, Q_j = \frac{1}{W_{mean-std}^j}. \quad (12) \\ U_j = e^{(W_{std}^j - W_{std}^k)^2}.$$

As shown in Table 3, for every strategy (Equation 3, 9, 10, 11, and 12), we experiment different Re-TCL methods which combine our TCL with different category-based grouping methods. Ours combining TCL with the strategy (in Equation 3) is better for few-shot detection.

**Impact of category-based grouping mechanism.** Without additional datasets, as detailed in Equation 3, we mainly focus on the similar appearance between different categories, followed by similar scenes, exploiting the relationships to promote performance. For Equation 3, we analyze category-based grouping, and compare with every ablation. As shown in Table 1, compared with only classification, splitting 20 categories into 6 disjoint groups can improve performance for few-shot detection.

**Impact on dispersion.** As shown in Table 2, Re-BCEwithLogits, Re-Focal, and Re-Cross-Entropy is compared with the BCEwithLogits, Focal, and Cross-Entropy, respectively. We find that the better meta-feature distribution between categories can alleviate the unbalanced performance on all categories. Especially for novel set1 2-shot, the dispersion of Re-Focal and Re-Cross-Entropy are reduced by 5.01% and 2.73%, respectively. Therefore, our category-based grouping mechanism can help distribution between similar semantic classes more compact and exploit the correlation between categories better. For novel set1 1-shot, 2-shot and 3-shot, ours which combines the TCL-2

Shot	Method	Novel Set 1						APs	
		boat	cat	mbike	sheep	sofa	mean	base AP	AP
1	Re-TCL (Equation 9 and 10)	9.39	<b>37.6</b>	28.63	17.93	12.84	<b>21.27</b>	65.72	54.61
	Re-TCL (Equation 9 and 11)	4.55	32.78	29.89	18.28	10.87	19.27	<b>66.51</b>	<b>54.7</b>
	Re-TCL (Equation 9 and 12)	9.09	34.75	21.63	17.11	<b>19.67</b>	20.45	65.14	53.97
	Ours 3	<b>9.53</b>	33.58	<b>32.28</b>	<b>19.66</b>	5.34	20.08	65.44	54.1
2	Re-TCL (Equation 9 and 10)	7.22	41.24	20.34	32.36	13.66	22.96	64.83	<b>55.61</b>
	Re-TCL (Equation 9 and 11)	5.22	39.38	<b>33.79</b>	33.46	11.9	24.75	65.05	54.97
	Re-TCL (Equation 9 and 12)	2.19	<b>45.05</b>	25.01	27.84	17.8	23.56	64.83	54.51
	Ours 3	<b>10.61</b>	35.11	33.75	<b>35.89</b>	<b>18.38</b>	<b>26.75</b>	<b>65.18</b>	55.58
3	Re-TCL (Equation 9 and 10)	6.32	<b>47.77</b>	22.45	27.92	29.99	26.89	65.55	55.89
	Re-TCL (Equation 9 and 11)	<b>10.46</b>	47.35	27.08	26.12	<b>37.72</b>	29.75	65.11	56.27
	Re-TCL (Equation 9 and 12)	10.29	39.55	18.76	28.67	33.84	26.22	65.18	55.44
	Ours 3	10.29	46.05	<b>28.11</b>	<b>29.81</b>	34.52	<b>29.76</b>	<b>65.64</b>	<b>56.67</b>

Table 3. The detection APs(%) on Pascal VOC by combining our TCL with different category-based grouping methods. For  $k$ -shot detection,  $k = 1, 2, 3$ , ours is better than others for novel set1. This table illustrates APs (i.e. every novel class, the mean AP on the novel classes, the mean AP on the base classes, and the mean AP on the all categories).

with the category-based grouping makes the lower dispersion on all categories, alleviating the strong bias problem.

As shown in Figure 4, for a subgraph, each category-based meta-feature is represented by different color histograms, and each subgraph is represented as a group with categories. We find that the meta-features distribution is very similar within a group, and the difference between groups is obvious. For dynamic weighting method, the category-based grouping method obtains each common meta-feature space between different categories within the group to improve the few-shot detection performance.

### 4.3. Visualization and Results

Our TCL- $C$  and category-based grouping can improve detection performance on few-shot, as seen in Appendix A. First, as detailed in Equation 1 and Figure 3 (a), our TCL-2 performs better for similar semantics to improve the detection APs on the novel classes.

Then, according to the similar appearance and environment which different categories appear, as detailed in Figure 1 and Equation 3, we split all categories into  $K$  groups which is disjoint each other. The distribution of meta-features is compact between categories within a group, the distribution between groups is far away from each other. That category-based grouping exploits similar distribution of category-based meta-features and reduces the detection dispersion on all categories, further improving performance. As can be seen from Figure 3 (a), Figure 4 and Table 2, the category-based grouping helps meta-model extract the shared meta-features between categories and ours improves the detection APs by similar semantics between categories. The method reduces the dispersion of the detection APs on all classes.

Combining TCL-2 with category-based grouping is more beneficial for few-shot detection. As shown in Table 1, for  $k$ -shot detection,  $k = 1, 2, 3$ , our method is better, and

the detection APs are close to 20.0%, 25%, 30%, respectively. For novel set3, the novel classes are "aero, bottle, cow, horse, sofa" and the remaining is the base classes. Although there is no novel class associated with the base categories, our method is 4.32%, 9.82% and 6.35% better than the BCEwithLogits, the Focal and Re-Cross-Entropy for novel set3 1-shot, respectively.

## 5. Conclusions

In this work, for few-shot detection, we present a TCL- $C$  for exploiting most similar class to improve the detection performance on novel (i.e. few-shot) classes, and a category-based grouping method for helping meta-model extract category-related meta-features better, alleviating the strong bias problem and further improving performance. Based on similar appearance or the environment they appeared, this paper splits categories into disjoint groups. This method helps the meta-model extract meta-feature vectors, making distribution of meta-features within a group more compact and difference of meta-features more obvious between groups. For 1-shot, 2-shot, and 3-shot detection, our method obtains all detection APs of almost 20%, 25%, and 30%. In the future, we will combine categories-embedded features and unsupervised clustering to group more categories, and apply the attention mechanism to improve performance for few-shot detection.

## References

- [1] Pieter Abbeel. A simple neural attentive meta-learner. 2
- [2] Antreas Antoniou, Harrison Edwards, and Amos Storkey. How to train your maml. *arXiv: Learning*, 2018. 3
- [3] Ankan Bansal, Karan Sikka, Gaurav Sharma, Rama Chellappa, and Ajay Divakaran. Zero-shot object detection. pages 397–414, 2018. 3
- [4] Nick Barnes. Polarity loss for zero-shot object detection. 2



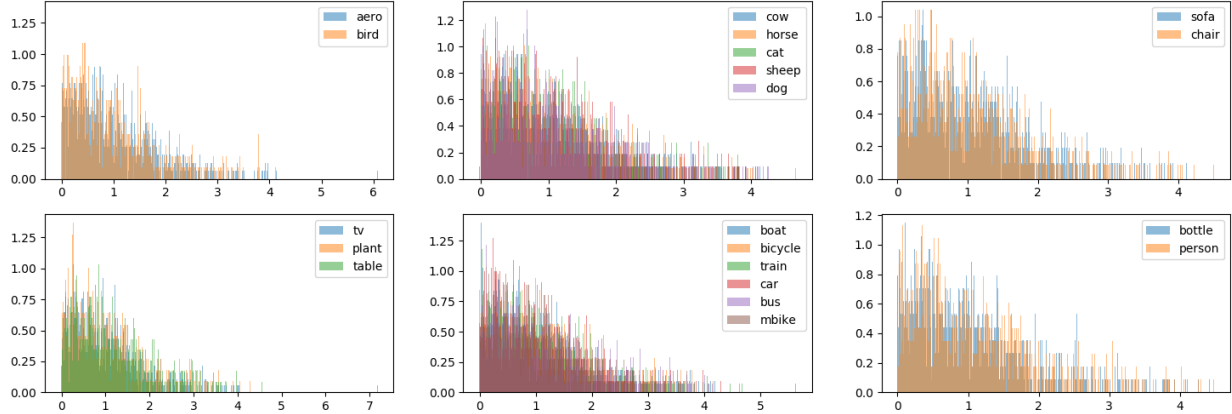


Figure 4. Histogram of meta-features distributions. The distribution of meta-feature vectors of 20 categories. In a sub-figure, the feature vectors of each group are represented, and different colors represent different categories within a group. Every meta-feature in a subgraph is very similar, and the distribution difference between subgraphs is obvious. Our method can extract shared meta-features within a group better.

- [5] Hakan Bilen and Andrea Vedaldi. Weakly supervised deep detection networks. pages 2846–2854, 2016. 3
- [6] Andrei Bursuc. Dense classification and implanting for few-shot learning. 1
- [7] Hao Chen, Yali Wang, Guoyou Wang, and Yu Qiao. Lstd: A low-shot transfer detector for object detection. pages 2836–2843, 2018. 3
- [8] Ajay Divakaran. Zero-shot object detection. 1
- [9] Xuanyi Dong, Liang Zheng, Fan Ma, Yi Yang, and Deyu Meng. Few-example object detection with model communication. *IEEE Transactions on Pattern Analysis and Machine Intelligence*, 41(7):1641–1654, 2019. 3
- [10] Qi Fan, Wei Zhuo, Chi-Keung Tang, and Yu-Wing Tai. Few-shot object detection with attention-rpn and multi-relation detector. In *Proceedings of the IEEE/CVF Conference on Computer Vision and Pattern Recognition*, pages 4013–4022, 2020. 3
- [11] Li Fei-Fei. Label efficient learning of transferable representations across domains and tasks. 2
- [12] Chelsea Finn, Pieter Abbeel, and Sergey Levine. Model-agnostic meta-learning for fast adaptation of deep networks. pages 1126–1135, 2017. 2
- [13] Chelsea Finn and Sergey Levine. Meta-learning and universality: Deep representations and gradient descent can approximate any learning algorithm. *arXiv: Learning*, 2017. 2
- [14] Ross Girshick. Low-shot visual recognition by shrinking and hallucinating features. 2
- [15] Erin Grant, Chelsea Finn, Sergey Levine, Trevor Darrell, and Thomas L Griffiths. Recasting gradient-based meta-learning as hierarchical bayes. *arXiv: Learning*, 2018. 2
- [16] Bharath Hariharan. Few-shot learning with localization in realistic settings. 1
- [17] Bharath Hariharan. Low-shot learning from imaginary data. 2
- [18] Martial Hebert. Watch and learn: Semi-supervised learning of object detectors from videos. 1, 3
- [19] Bingyi Kang, Zhuang Liu, Xin Wang, Fisher Yu, Jiashi Feng, and Trevor Darrell. Few-shot object detection via feature reweighting. pages 8420–8429, 2019. 2, 3, 6
- [20] Junsik Kim, Taehyun Oh, Seokju Lee, Fei Pan, and In So Kweon. Variational prototyping-encoder: One-shot learning with prototypical images. *arXiv: Computer Vision and Pattern Recognition*, 2019. 2
- [21] Tao Kong, Fuchun Sun, Huaping Liu, Yuning Jiang, and Jianbo Shi. Foveabox: Beyond anchor-based object detector. *arXiv preprint arXiv:1904.03797*, 2019. 1
- [22] Yoonho Lee and Seungjin Choi. Gradient-based meta-learning with learned layerwise metric and subspace. pages 2927–2936, 2018. 2
- [23] Wenbin Li, Lei Wang, Jinglin Xu, Jing Huo, Yang Gao, and Jiebo Luo. Revisiting local descriptor based image-to-class measure for few-shot learning. pages 7260–7268, 2019. 2
- [24] Yann Lifchitz, Yannis Avrithis, Sylvaine Picard, and Andrei Bursuc. Dense classification and implanting for few-shot learning. pages 9258–9267, 2019. 2
- [25] Tsung Yi Lin, Priyal Goyal, Ross Girshick, Kaiming He, and Piotr Dollar. Focal loss for dense object detection. *IEEE Transactions on Pattern Analysis & Machine Intelligence*, PP(99):2999–3007, 2017. 2, 5, 6
- [26] Weiyang Liu, Yandong Wen, Zhiding Yu, Ming Li, Bhiksha Raj, and Le Song. Sphreface: Deep hypersphere embedding for face recognition. pages 6738–6746, 2017. 2
- [27] Weiyang Liu, Yandong Wen, Zhiding Yu, and Meng Yang. Large-margin softmax loss for convolutional neural networks. *arXiv: Machine Learning*, 2016. 2
- [28] Alex Nichol, Joshua Achiam, and John Schulman. On first-order meta-learning algorithms. *arXiv: Learning*, 2018. 3
- [29] Boris N Oreshkin, Pau Rodriguez Lopez, and Alexandre Lacoste. Tadam: Task dependent adaptive metric for improved few-shot learning. pages 721–731, 2018. 2
- [30] Pedro O Pinheiro. Adaptive cross-modal few-shot learning. 1, 2

- [31] Fatih Porikli. Zero-shot object detection: Learning to simultaneously recognize and localize novel concepts. 1, 3
- [32] Joseph Redmon, Santosh Divvala, Ross Girshick, and Ali Farhadi. You only look once: Unified, real-time object detection. 2015. 1
- [33] Joseph Redmon and Ali Farhadi. Yolo9000: Better, faster, stronger. In *IEEE Conference on Computer Vision & Pattern Recognition*, 2017. 1, 2, 3
- [34] Shaoqing Ren, Kaiming He, Ross Girshick, and Jian Sun. Faster r-cnn: Towards real-time object detection with region proposal networks. *IEEE Transactions on Pattern Analysis & Machine Intelligence*, 39(6):1137–1149, 2017. 3
- [35] Reuven Rubinstein. The cross-entropy method for combinatorial and continuous optimization. *Methodology & Computing in Applied Probability*, 2(2):127–190, 1999. 2, 5, 6
- [36] Andrei A Rusu, Dushyant Rao, Jakub Sygnowski, Oriol Vinyals, Razvan Pascanu, Simon Osindero, and Raia Hadsell. Meta-learning with latent embedding optimization. 2019. 3
- [37] Venkatesh Saligrama. Zero-shot detection. *IEEE Transactions on Circuits & Systems for Video Technology*. 1
- [38] Adam Santoro, Sergey Bartunov, Matthew Botvinick, Daan Wierstra, and Timothy Lillicrap. Meta-learning with memory-augmented neural networks. pages 1842–1850, 2016. 2
- [39] Mubarak Shah. Task-agnostic meta-learning for few-shot learning. 1
- [40] Hyun Oh Song, Yong Jae Lee, Stefanie Jegelka, and Trevor Darrell. Weakly-supervised discovery of visual pattern configurations. pages 1637–1645, 2014. 3
- [41] Qianru Sun, Yaoyao Liu, Tatseng Chua, and Bernt Schiele. Meta-transfer learning for few-shot learning. pages 403–412, 2019. 3
- [42] Zhi Tian, Chunhua Shen, Hao Chen, and Tong He. FCOS: Fully convolutional one-stage object detection. In *Proc. Int. Conf. Computer Vision (ICCV)*, 2019. 1
- [43] Luc Van Gool. Weakly supervised cascaded convolutional networks. 2017. 3
- [44] Yuxiong Wang and Martial Hebert. Model recommendation: Generating object detectors from few samples. pages 1619–1628, 2015. 3
- [45] Davis Wertheimer and Bharath Hariharan. Few-shot learning with localization in realistic settings. pages 6558–6567, 2019. 2
- [46] Haiyong Xie. Dual adversarial semantics-consistent network for generalized zero-shot learning. 1, 2
- [47] Richard S Zemel. Incremental few-shot learning with attention attractor networks. 2

Shot	Method	Novel					Base																
		boat	cat	mbike	sheep	sofa	mean	aero	bike	bird	bottle	bus	car	chair	cow	table	dog	horse	person	plant	train	tv	mean
1	YOLO-joint	0.0	9.1	0.0	0.0	0.0	1.8	78.7	76.8	73.4	48.8	79.0	82.3	50.2	68.4	71.4	76.7	80.7	75.0	46.8	83.8	71.7	70.9
	YOLO-ft	0.1	25.8	10.7	3.6	0.1	8.1	77.2	74.9	69.1	47.4	78.7	79.7	47.9	68.3	69.6	74.7	79.4	74.2	42.2	82.7	71.1	69.1
	YOLO-ft-full	0.1	30.9	26.0	8.0	0.1	13.0	75.1	70.7	65.9	43.6	78.4	79.5	47.8	68.7	68.0	72.8	79.5	72.3	40.1	80.5	68.6	67.4
	<b>Baseline</b>	10.8	44.0	17.8	18.1	5.3	19.2	77.1	71.8	66.3	40.4	75.2	77.8	50.1	54.6	66.8	69.1	78.3	68.1	41.9	80.6	70.3	65.9
	BCewithLogits	9.09	22.3	25.47	15.56	9.67	16.42	71.91	73.19	62.09	42.19	72.81	76.81	46.55	51.06	63.8	66.6	77.99	67.24	40	80.42	69.46	64.11
	Re-BCewithLogits	2.6	23.81	19.89	19.76	0.22	13.26	71.61	72.1	66.8	41.64	74.47	75.84	46.48	57.61	66.5	68.8	79.13	70.27	40.78	78.62	69.68	65.36
	Focal	1.55	<b>42.88</b>	15.23	16.72	4.98	16.27	75.89	72.62	71.47	43.01	78.7	76.87	48.79	53.16	62.29	71.2	79.33	71.7	38.22	77.16	68.65	65.94
	Re-Focal	<b>9.79</b>	37.99	20.64	<b>20.14</b>	2.54	18.22	75.27	71.74	66.44	41.01	75.73	76.07	46.39	52.88	63.02	69.68	81.9	70.64	38.75	80.53	68.17	65.22
	Cross-Entropy	3.52	29.01	25.6	16.43	2.27	15.37	71.6	72.08	65.53	39.42	75.42	76.06	43.93	57.07	64.87	68.09	78.69	69.24	37.81	78.67	68.35	64.45
	Re-Cross-Entropy	9.52	33.67	27.33	12.35	9.85	18.55	73.86	74.4	66.14	40.42	73.87	76.45	47.09	53.91	68.13	70.78	78.2	67.53	35.64	76.24	67.65	64.69
2	TCL-2	6.43	33.8	31.21	11.51	<b>12.8</b>	19.15	72.03	71	67.24	42.16	74.23	76.77	46.57	54.34	65.69	71.61	81.02	69.77	41.35	77.03	69.46	65.35
	<b>Ours</b>	9.53	33.58	<b>32.28</b>	19.66	5.34	<b>20.08</b>	71.98	72.65	65.45	41.96	75.14	78.44	43.75	52.03	65.04	73.27	80.29	68.78	43.46	80.36	68.97	65.44
	YOLO-joint	0.0	9.1	0.0	0.0	0.0	1.8	77.6	77.1	74.0	49.4	79.8	79.9	50.5	71.0	72.7	76.3	81.0	75.0	48.4	84.9	72.7	71.4
	YOLO-ft	0.0	24.4	2.5	9.8	0.1	7.4	78.2	76.0	72.2	47.2	79.3	79.8	47.3	72.1	70.0	74.9	80.3	74.3	45.2	84.9	72.0	70.2
	YOLO-ft-full	0.0	35.2	28.7	15.4	0.1	15.9	75.3	72.0	69.8	44.0	79.1	78.8	42.1	70.0	64.9	73.8	81.7	71.4	40.9	80.9	69.4	67.6
	<b>Baseline</b>	5.3	46.4	18.4	26.1	12.4	21.7	71.4	72.4	64.5	37.9	75.3	77.1	42.9	55.0	57.4	73.7	78.9	68.0	41.5	75.9	69.0	64.1
	BCewithLogits	4.57	30.21	23.74	17.66	16.36	18.51	69.8	71.62	62.79	40.77	73.2	77.57	46.19	55.03	64.48	67.55	78.61	68.79	39.37	74.09	66.16	63.74
	Re-BCewithLogits	2.93	28.84	19.64	27.16	8.74	17.46	71.5	72.77	68.1	40.92	74.89	75.99	42.6	58.7	65.78	67.99	79.35	69.94	40.27	73.78	66.97	64.64
	Focal	2.58	<b>43.85</b>	11.29	33.16	17.29	21.63	72.16	71.4	69.1	42.31	75.8	73.5	44.85	61.52	64.11	70.09	79.28	70	39.02	78.23	69.14	65.37
	Re-Focal	6.15	33.6	18.95	29.43	12.1	20.05	74.88	62.18	66.6	41.13	76.91	76.51	45.4	60.88	62.23	70.71	82.32	71.68	42.19	74.26	67.51	65.03
3	Cross-Entropy	10.25	36.46	16.2	24.97	7.66	19.11	72.31	75.59	67.87	40.79	74.26	76.95	42.75	59.03	66.24	72.86	79.03	71.4	39.73	75.37	67.32	65.43
	Re-Cross-Entropy	10.06	38.83	19.41	17.65	<b>19.15</b>	21.02	70.92	73.33	66.49	38.73	74.36	75.59	46.96	59.51	66.33	70.34	78.13	70.29	40.36	69.74	67.04	64.54
	TCL-2	4.95	32.49	28.31	27.06	13.34	21.23	60.79	70.66	67.51	39.37	74.61	76.4	39.26	54.21	66.68	70.81	79.91	69.22	41.68	67.71	67.89	63.71
	<b>Ours</b>	<b>10.61</b>	35.11	<b>33.75</b>	<b>35.89</b>	18.38	<b>26.75</b>	70.53	73.53	66.6	43.18	75.52	77.71	41.29	53.9	63.63	72.5	80.85	69.77	43.08	77.27	68.42	65.18
	YOLO-joint	0.0	9.1	0.0	0.0	0.0	1.8	77.1	77.0	70.6	46.3	77.5	79.7	49.7	68.8	73.4	74.5	79.4	75.6	48.1	83.6	72.1	70.2
	YOLO-ft	0.0	27.0	1.8	9.1	0.1	7.6	77.7	76.6	71.4	47.5	78.0	79.9	47.6	70.0	70.5	74.4	80.0	73.7	44.1	83.0	70.9	69.7
	YOLO-ft-full	0.0	39.0	18.1	17.9	0.0	15.0	73.2	71.1	68.8	43.7	78.9	79.3	43.1	67.8	62.2	76.3	79.4	70.8	40.5	81.6	69.6	67.1
	<b>Baseline</b>	11.2	39.8	20.9	23.7	33.0	25.7	73.2	68.0	65.9	39.8	77.3	77.5	43.5	57.7	60.7	64.5	77.5	68.4	42.0	80.6	70.2	64.4
	BCewithLogits	<b>10.92</b>	<b>46.62</b>	24.57	23.23	31.71	27.41	73.06	71.22	62.71	40.1	73.9	77.79	46.02	55.06	62.75	67.95	79.51	65.49	39.81	76.69	67.36	63.96
	Re-BCewithLogits	9.77	45.18	22.77	22.37	21.47	24.31	71.95	70.14	63.95	38.09	74.65	74.86	41.02	57.12	58.25	63.08	79.29	65.36	40.36	73.38	67.43	62.6
5	Focal	10.36	43.77	19.45	28.41	<b>37.56</b>	27.91	72.71	71.66	66.84	42.79	76.13	76.71	44.92	57.42	66.61	68	81.97	68.8	40.25	77.19	67.44	65.3
	Re-Focal	11.67	27.17	16.83	30.07	16.52	20.45	73.75	72.52	69.66	43.83	76.44	77.94	48.14	64.6	66.78	71.62	83.64	70.66	43.86	79.86	68.55	67.32
	Cross-Entropy	7.42	32.57	14.75	<b>31.04</b>	29.76	23.11	70.8	73.39	69.21	40.52	75.33	78.98	46.07	57.42	66.21	69.44	79.53	69.03	38.8	79.15	65.43	65.29
	Re-Cross-Entropy	10.47	32.89	16.06	24.1	28.75	22.25	74.1	74.44	68	41.23	77.62	76.84	48.19	58.56	67.15	69.26	78.71	69.84	38.12	80.31	67.1	65.96
	TCL-2	9.67	47.2	25.11	28.97	32.26	28.64	72.5	67.82	67.63	39.08	75.28	77.06	43.79	53.3	65.71	72.9	80.65	69.11	41.24	76.85	69.16	64.8
	<b>Ours</b>	10.29	46.05	<b>28.11</b>	29.81	34.52	<b>29.76</b>	72.45	73.14	66.32	41.18	75.07	78.55	45.04	56.81	64.46	72.73	81.23	68.26	42.61	79.87	66.89	65.64
	YOLO-joint	0.0	9.1	0.0	0.0	9.1	3.6	78.2	78.5	72.1	47.8	76.6	82.1	50.7	70.1	71.8	77.6	80.4	75.4	46.0	84.8	72.5	71.0
	YOLO-ft	0.0	33.8	2.6	7.8	3.2	9.5	77.2	77.1	71.9	47.3	78.8	79.8	47.1	69.8	71.8	77.0	80.2	74.3	44.2	82.5	70.6	70.0
	YOLO-ft-full	7.9	48.0	39.1	29.4	36.6	32.2	75.5	73.6	69.1	43.3	78.4	78.9	42.3	70.2	66.1	77.4	79.8	72.2	41.9	82.8	69.3	68.1
	<b>Baseline</b>	<b>14.2</b>	<b>57.3</b>	<b>50.8</b>	38.9	41.6	<b>40.6</b>	70.1	66.3	66.5	40.0	78.1	77.0	40.4	61.2	61.5	71.2	79.1	70.4	38.5	80.0	68.0	64.6
5	BCewithLogits	8.91	49.65	49.11	31.72	40.95	36.07	70.68	73.05	65.16	38.42	75	77.82	41.25	61.02	62.72	71.88	79.94	68.33	40.99	77.75	67.68	64.78
	Re-BCewithLogits	12.61	44.16	42.49	36.93	32.59	33.76	70.83	73.53	67.28	38.7	76.79	76.65	39.31	64.76	63.29	69.56	81.21	66.78	39.42	78.28	68.1	64.97
	Focal	8.04	52.42	48.07	39.9	38.76	37.43	72.2	72.54	66.31	40.65	78.69	76.74	43.54	64.5	68.53	69.94	81.07	69.84	37.68	80.03	69.13	66.09
	Re-Focal	12.66	42.89	43.28	<b>40.7</b>	<b>43.44</b>	36.15	73.2	66.09	66.03	41.02	77.06	76.78	44.6	65.74	63.48	67.93	82.62	70.46	40.7	76.88	68.1	65.38
	Cross-Entropy	7.37	45.65	44.55	39.62	38.7	35.18	72.32	69.03	67.67	40.15	77.41	77.16	40.29	60.94	64.86	73.51	81.17	69.68	38.94	80.75	67.45	65.42
	Re-Cross-Entropy	10.66	48.92	44.25	36.05	42.65	36.5	75.5	75.17	69.9	40.72	77.28	76.96	47.54	62.26	65.63	73.91	79.66	70.86	38.87	80.68	68.61	66.9
	TCL-2	5.94	55.34	49.25	34.84	39.33	36.94	70.44	66.41	64.71	35.75	75.56	75.54	35.72	59.05	57.86	73.47	77.87	66.64	37	75.44	65.73	62.48
	<b>Ours</b>	9.02	47.13	<b>49.78</b>	40.11	35.37	36.28	73.28	74.77	67.25	39.4	76.51	78.53	44.52	57.32	66.44	75.54	81.33	58.92	39.8	80.15	68.98	66.18

Table 4. The results of detection APs (%). For few-shot detection on Pascal VOC, ours significantly outperforms others on novel set1.

## A. Results and Visualization on Pascal VOC

For novel set 1, 2, 3, this section shows our all results for  $k$ -shot detection,  $k = 1, 2, 3, 5$ . Finally, we visualize all results on all novel categories (i.e. boat, cat, mbike, sheep and sofa) for novel set1 2-shot.

Shot	Method	Novel						Base															
		bird	bus	cow	mbike	sofa	mean	aero	bike	boat	bottle	car	cat	chair	table	dog	horse	person	plant	sheep	train	tv	mean
1	YOLO-joint	0.0	0.0	0.0	0.0	0.0	0.0	78.4	76.9	61.5	48.7	79.8	84.5	51.0	72.7	79.0	77.6	74.9	48.2	62.8	84.8	73.1	70.2
	YOLO-ft	6.8	0.0	9.1	0.0	0.0	3.2	77.1	78.2	61.7	46.7	79.4	82.7	51.0	69.0	78.3	79.5	74.2	42.7	68.3	84.1	72.9	69.7
	YOLO-ft-full	11.4	17.6	3.8	0.0	0.0	6.6	75.8	77.3	63.1	45.9	78.7	84.1	52.3	66.5	79.3	77.2	73.7	44.0	66.0	84.2	72.2	69.4
	<b>Baseline</b>	13.5	10.6	31.5	13.8	4.3	14.8	75.1	70.7	57.0	41.6	76.6	81.7	46.6	72.4	73.8	76.9	68.8	43.1	63.0	78.8	69.9	66.4
	BCEwithLogits	10.56	17.23	5.64	<b>33.62</b>	0.91	13.59	74.13	69.35	54.19	38.89	75.62	80.05	48.07	61.85	72.03	74.75	64.59	38.88	58.63	77.72	68.27	63.8
	Re-BCEwithLogits	5.89	38.39	14.65	32.00	0.51	<b>18.29</b>	73.1	69.84	55.76	40.42	76.81	78.51	46.1	63.73	75.78	77.92	68.69	40.41	59.85	79.28	70.79	65.13
	Focal	11.18	1.17	13.66	25.83	0.1	10.39	74.61	73.96	53.91	41.82	53.8	78.28	48.87	24.36	78.16	76.08	71.31	42.12	64.13	81.33	70.97	62.25
	Re-Focal	11.41	6.89	22.09	28.55	1.89	14.16	72.78	69.65	55.88	40.02	77.14	82.69	47.32	67.15	78.6	77.33	68.6	40.36	62.98	80.14	70.69	66.09
	Cross-Entropy	12.49	11.16	<b>24.72</b>	28.79	3.03	16.04	72.85	69.98	55.87	43.31	76.53	77.72	45.37	69.87	75.76	75.98	69.72	40.07	59.27	78.15	70.13	65.37
	Re-Cross-Entropy	12.35	16.28	13.23	33.41	0.47	15.15	73.02	70.19	60.02	41.78	77.59	80.05	44.86	66.17	78.08	75.95	70	40	59.47	79.68	68.27	65.68
	TCL-2	18.21	18.02	15.38	24.2	<b>11.99</b>	17.56	69.95	72.15	55.51	37.15	76.74	81.57	45.66	68.99	72.95	75.79	68.26	41.47	62.86	78.64	70.91	65.24
	<b>Ours</b>	<b>19.18</b>	<b>22.58</b>	7.62	30.81	10.16	18.07	72.43	76.21	56.25	40.45	77.07	81.02	47.89	67.63	75.06	74.2	69.72	39.38	61.51	76.96	67.46	65.55
2	YOLO-joint	0.0	0.0	0.0	0.0	0.0	0.0	77.6	77.6	60.4	48.1	81.5	82.6	51.5	72.0	79.2	78.8	75.2	47.0	65.2	86.0	72.7	70.4
	YOLO-ft	11.5	5.8	7.6	0.1	7.5	6.5	77.9	75.0	58.5	45.7	77.6	84.0	50.4	68.5	79.2	79.7	73.8	44.0	66.0	77.5	72.9	68.7
	YOLO-ft-full	16.6	9.7	12.4	0.1	14.5	10.7	76.4	70.2	56.9	43.3	77.5	83.8	47.8	70.7	79.1	77.6	71.7	39.6	61.4	77.0	70.3	66.9
	<b>Baseline</b>	21.2	12.0	16.8	17.9	9.6	15.5	74.6	74.9	56.3	38.5	75.5	68.0	43.2	69.3	66.2	42.4	68.1	41.8	59.4	76.4	70.3	61.7
	BCEwithLogits	19.22	12.11	21.55	14.98	5.7	14.71	71.83	70.38	54.28	37.96	75.46	81.24	44.12	71.37	77.53	76.8	69.95	39.44	54.8	72.74	66.68	64.3
	Re-BCEwithLogits	15.18	6.49	27.69	26.89	<b>22.27</b>	19.71	72.21	72.97	55.33	39.56	74.71	77.94	43.68	65.32	77.86	77.43	68.3	39.71	57.31	76.16	68.11	64.44
	Focal	19.13	11.25	28.13	15.09	2.56	15.23	74.46	77.02	54.96	43.77	77.86	82.33	45.03	68.47	79.01	75.34	72.02	43.38	62.98	79.66	68.55	66.99
	Re-Focal	12.45	3.88	37.62	19.14	6.28	15.88	72.29	72.52	59.1	44.79	78.15	82.47	47.14	68.25	79.49	76.44	72.27	41.79	67.79	75.44	69.9	67.19
	Cross-Entropy	24.64	7.22	27.93	27.00	9.19	19.2	74.52	70.24	55.12	42.94	77.14	78.71	44.82	69.75	76.92	69.73	69.15	41.45	58.8	73.04	68.76	64.74
	Re-Cross-Entropy	23.43	11.61	19.13	<b>37.85</b>	12.04	20.81	71.79	70.63	59.38	41.65	77.42	81.35	44.56	66.39	78.41	56.23	70.88	40.77	52.71	73.85	68.52	63.64
	TCL-2	23.02	8.3	<b>36.51</b>	27.34	16.09	22.25	72.65	70.28	54.02	36.6	76.41	80.82	42.55	67.26	75.97	77.13	69.15	41.8	60.92	73.06	68.71	64.49
	<b>Ours</b>	<b>25.18</b>	<b>12.29</b>	31.87	32.71	21.23	<b>24.66</b>	72.31	73.62	55.07	38.23	74.73	81.85	44.37	65.41	75.94	75.85	69.93	39.81	56.93	73.31	65.72	64.21
3	YOLO-joint	0	0	0	0	9.1	1.8	78.0	77.2	61.2	45.6	81.6	83.7	51.7	73.4	80.7	79.6	75.0	45.5	65.6	83.1	72.7	70.3
	YOLO-ft	10.9	5.5	15.3	0.2	0.1	6.4	76.7	77.0	60.4	46.9	78.8	84.9	51.0	68.3	79.6	78.7	73.1	44.5	67.6	83.6	72.4	69.6
	YOLO-ft-full	21.0	22.0	19.1	0.5	0.0	12.5	73.4	67.5	56.8	41.2	77.1	81.6	45.5	62.1	74.6	78.9	67.9	37.8	54.1	76.4	71.9	64.4
	<b>Baseline</b>	26.1	19.1	40.7	20.4	27.1	26.7	73.6	73.1	56.7	41.6	76.1	78.7	42.6	66.8	72.0	77.7	68.5	42.0	57.1	74.7	70.7	64.8
	BCEwithLogits	24.71	22.63	29.19	<b>29.22</b>	25.75	26.3	71.62	70.05	54.66	37.51	75.44	79.7	46.09	63.79	75.58	77.37	67.16	40.1	49.63	73.3	66.12	63.21
	Re-BCEwithLogits	23.03	<b>29.91</b>	22.74	19.06	40.2	26.99	70.37	72.92	56.98	37.24	75.72	79.38	45.12	66.07	74.99	78.59	65.85	40.35	49.45	77.29	68.68	63.93
	Focal	10.3	16.38	33.76	17.11	14.24	18.36	73.33	74.27	55.78	43.21	79.32	82.48	47.69	70.4	76.97	79.0	70.32	42.39	61.53	81.29	70.48	67.23
	Re-Focal	25.98	11.44	37.02	20.43	20.79	23.13	72.58	70.06	58.43	42.27	78.28	80.97	47.52	66.97	78.47	76.03	68.9	41.7	60.5	75.51	69.02	65.81
	Cross-Entropy	28.17	14.07	32.98	24.2	27.86	25.46	73.07	70.39	56.28	41.02	73.88	80.17	45.97	70.5	75.79	77.58	68.22	40.2	55.15	76.83	69.07	64.94
	Re-Cross-Entropy	23.25	18.64	<b>37.54</b>	24.33	26.62	26.07	70.03	71.94	56.92	40.92	77.53	81.16	47.0	68.24	76.68	77.33	69.29	41.12	51.47	77.53	69.22	65.09
	TCL-2	31.15	23.29	23.97	19.96	29.49	25.57	67.69	66.26	51.65	35.66	76.84	80.62	45.79	66.01	74.73	77.15	65.55	40.55	57.96	77.71	69.72	63.59
	<b>Ours</b>	<b>32.1</b>	20.53	30.64	28.52	<b>42.9</b>	<b>30.94</b>	71.19	69.39	51.81	37.66	76.41	81.63	45.39	64.51	75.41	76.11	69.45	39.09	54.88	75.38	67.9	63.75
5	YOLO-joint	0.0	0.0	0.0	0.0	9.1	1.8	77.8	76.4	65.7	45.9	79.5	82.3	50.4	72.5	79.1	79.0	75.5	47.9	67.2	83.0	72.5	70.3
	YOLO-ft	11.6	7.1	10.7	2.1	6.0	7.5	76.5	76.4	61.0	45.5	78.7	84.5	49.2	68.7	78.5	78.1	73.7	45.4	66.8	85.3	70.0	69.2
	YOLO-ft-full	20.2	20.0	22.4	36.4	24.8	24.8	72.0	70.6	60.7	42.0	76.8	84.2	47.7	63.7	76.9	78.8	72.1	42.2	61.1	80.8	69.9	66.6
	<b>Baseline</b>	31.5	21.1	39.8	40.0	37.0	33.9	69.3	57.5	56.8	37.8	74.8	82.8	41.2	67.3	74.0	77.4	70.9	40.9	57.3	73.5	69.3	63.4
	BCEwithLogits	30.15	24.25	32.32	52.43	36.83	35.2	70.62	71.46	54.45	38.34	75.34	80.7	47.78	65.24	73.84	77.03	65.86	36.92	48.75	73.89	65.78	63.07
	Re-BCEwithLogits	25.41	36.34	25.49	46.96	<b>42.29</b>	35.3	69.14	74.33	55.5	37.18	76.77	79.12	45.9	64.79	76.47	77.61	67.74	38.64	53.98	78.21	68.97	64.29
	Focal	28.07	20.89	40.79	49.65	31.03	34.09	73.52	68.13	56.93	39.23	76.85	80.54	44.15	67.99	77.37	75.21	69.25	40.05	59.0	78.25	70.47	65.13
	Re-Focal	18.82	21.87	38.92	33.81	22.6	27.2	73.12	73.52	60.79	42.24	78.96	83.06	49.59	68.32	79.09	77.7	71.54	41.5	66.99	80.1	70.96	67.83
	Cross-Entropy	<b>33.26</b>	25.01	<b>40.64</b>	38.19	42.11	35.84	71.91	70.27	58.51	40.01	76.6	80.33	45.54	69.93	78.19	77.44	70.96	40.05	58.74	80.47	69.78	65.92
	Re-Cross-Entropy	29.4	14.81	37.89	49.28	35.85	33.45	70.98	70.31	56.94	41.35	77.53	83.88	45.11	67.13	76.83	78.14	70.17	41.45	56.7	76.74	67.41	65.38
	TCL-2	29.84	<b>42.46</b>	30.11	48.26	41.58	38.45	67.27	60.54	52.2	32.59	74.41	81.03	33.61	62.9	67.29	75.62	64.23	32.44	56.2	71.65	66.99	59.93
	<b>Ours</b>	30.35	37.51	30.7	<b>55.16</b>	41.49	<b>39.04</b>	67.82	67.17	48.47	33.66	73.42	78.18	39.45	61.11	69.54	74.0	68.07	36.5	55.67	71.31	65.04	60.63

Table 5. The results of detection APs (%). For few-shot detection on Pascal VOC, ours significantly outperforms others on novel set2.



Shot	Method	Novel						Base															
		aero	bottle	cow	horse	sofa	mean	bike	bird	boat	bus	car	cat	chair	table	dog	mbike	person	plant	sheep	train	tv	mean
1	YOLO-joint	0.0	0.0	0.0	0.0	0.0	0.0	78.8	73.2	63.6	79.0	79.7	87.2	51.5	71.2	81.1	78.1	75.4	47.7	65.9	84.0	73.7	72.7
	YOLO-ft	0.4	0.2	10.3	29.8	0.0	8.2	77.9	70.2	62.2	79.8	79.4	86.6	51.9	72.3	77.1	78.1	73.9	44.1	66.6	83.4	74.0	71.8
	YOLO-ft-full	0.6	9.1	11.2	41.6	0.0	12.5	74.9	67.2	60.1	78.8	79.0	83.8	50.6	72.7	75.5	74.8	71.7	43.9	62.5	81.8	72.6	70.0
	<b>Baseline</b>	11.8	9.1	15.6	23.7	18.2	15.7	77.6	62.7	54.2	75.3	79.0	80.0	49.6	70.3	78.3	78.2	68.5	42.2	58.2	78.5	70.4	68.2
	BCEwithLogits	10.12	0.7	7.86	39.72	<b>17.1</b>	15.1	74.81	64.83	52.22	73.61	76.19	78.31	46.72	66.34	78.4	77.34	67.81	37.57	58.53	74.82	70.73	66.55
	Re-BCEwithLogits	10.74	0.51	7.39	31.33	5.05	11	73.86	62.79	49.72	72.46	77.28	80.37	44.56	66.54	76.61	75.87	65.98	38.26	57.72	71.58	68.98	65.5
	Focal	10.76	0.06	16.13	19.98	1.06	9.6	75.75	65.05	57.9	77.11	77.29	81.48	46.04	62.73	75.47	74.19	69.38	40.55	54.75	78.08	69.18	67
	Re-Focal	9.48	0.03	19.36	7.48	0.13	7.3	78.53	68.12	59.02	77.91	78.58	83.09	50.56	57.57	72.67	76.19	69.51	42.75	59.86	72.39	70.87	67.8
	Cross-Entropy	14.01	0.34	10.89	25.89	9.88	12.19	73.46	62.63	52.58	74.92	76.8	81.12	46.33	66.23	79.3	74.31	68.15	38.79	56.06	76.86	69.38	66.46
	Re-Cross-Entropy	9.28	0.22	<b>21.57</b>	25.2	9.09	13.07	75.33	64.84	54.94	75.81	77.84	82.48	47.64	63.8	78.3	75.53	70.4	38.38	57.96	76.01	67.7	67.13
	TCL-2	0.76	0.07	16.96	29.59	13.99	12.27	75.82	60.6	54.09	75.65	77.95	84.08	48.81	64.8	73.36	77.1	71.26	40.53	58.01	78.17	69.27	67.3
	<b>Ours</b>	<b>16.33</b>	<b>9.09</b>	8.7	<b>46.9</b>	16.08	<b>19.42</b>	72.71	62.94	45	74.97	75.29	77.39	44.73	64.71	67.84	74.99	68.65	38.36	54.3	76.09	68.95	64.46
2	YOLO-joint	0.0	0.6	0.0	0.0	0.0	0.1	78.4	69.7	64.5	78.3	79.7	86.1	52.2	72.6	81.2	78.6	75.2	50.3	66.1	85.3	74.0	72.8
	YOLO-ft	0.2	0.2	17.2	1.2	0.0	3.8	78.1	70.0	60.6	79.8	79.4	87.1	49.7	70.3	80.4	78.8	73.7	44.2	62.2	82.4	74.9	71.4
	YOLO-ft-full	1.8	1.8	15.5	1.9	0.0	4.2	76.4	69.7	58.0	80.0	79.0	86.9	44.8	68.2	75.2	77.4	72.2	40.3	59.1	81.6	73.4	69.5
	<b>Baseline</b>	28.6	0.9	27.6	0.0	19.5	15.3	75.8	67.4	52.4	74.8	76.6	82.5	44.5	66.0	79.4	76.2	68.2	42.3	53.8	76.6	71.0	67.2
	BCEwithLogits	28.39	0.61	28.6	0.53	<b>19.97</b>	15.62	74.24	67.99	51.14	75.32	76.18	79.04	45.98	66.83	77.66	77.48	68.75	38.91	55.13	75.69	70.05	66.69
	Re-BCEwithLogits	21.59	0.22	25.02	0.19	17.96	13	75.95	64.26	48.5	76.34	77.12	81.84	43.76	67.99	78.27	76.22	68.65	42.37	54.22	76.54	68.03	66.67
	Focal	26.74	<b>1.3</b>	13.04	0.66	2.59	8.87	73.85	67.33	54.91	77.18	78.56	82.54	44.52	63.84	80.36	77.87	69.33	42.3	58.35	77.97	69.95	67.92
	Re-Focal	14.44	0.29	24.55	0.13	3.94	8.67	77.32	70.66	56.19	78.09	78.07	83.41	48.05	65.54	79.71	78.13	68.42	42.57	59.41	76.83	70.55	68.86
	Cross-Entropy	28.6	0.9	27.6	0	19.5	15.3	75.8	67.4	52.4	74.8	76.6	82.5	44.5	66	79.4	76.2	68.2	42.3	53.8	76.6	71	67.2
	Re-Cross-Entropy	28.4	0.13	28.42	0.57	15.15	14.53	75.4	67.05	57.57	75.18	77.82	82.17	49.28	71.61	79.59	76.72	70.17	42.48	59.89	76.29	68.35	68.64
	TCL-2	<b>34.66</b>	0.83	31.32	1.01	18.82	17.33	69.88	61.47	50.09	72.15	73.96	77.26	38.45	61.21	73.48	74.39	66.28	37	50.94	71.34	66.07	62.93
	<b>Ours</b>	34.14	0.49	<b>34.6</b>	<b>2.27</b>	15.65	<b>17.43</b>	77.56	65.59	51.74	72.95	76.14	79.49	42.88	64.67	76.65	75.98	70.37	41.08	55.8	75.15	68.4	66.3
3	YOLO-joint	0.0	0.0	0.0	0.0	0.0	0.0	77.6	72.2	61.2	77.9	79.8	85.8	49.9	73.2	80.0	77.9	75.3	50.8	64.3	84.2	72.6	72.2
	YOLO-ft	4.9	0.0	11.2	1.2	0.0	3.5	78.7	71.6	62.4	77.4	80.4	87.5	49.5	70.8	79.7	79.5	72.6	44.3	60.0	83.0	75.2	71.5
	YOLO-ft-full	10.7	4.6	12.9	29.7	0.0	11.6	74.9	69.2	60.4	79.4	79.1	87.3	43.4	69.7	75.8	75.2	70.5	39.4	52.9	80.8	73.4	68.8
	<b>Baseline</b>	29.4	4.6	34.9	6.8	37.9	22.7	62.6	64.7	55.2	76.6	77.1	82.7	46.7	65.4	75.4	78.3	69.2	42.8	45.2	77.9	69.6	66.0
	BCEwithLogits	32.19	9.09	29.2	18.99	<b>41.25</b>	26.14	71.29	64.92	50.96	75.89	76.87	80.89	47.81	67.03	75.62	75.87	65.67	37.94	40.8	78.44	70.66	65.38
	Re-BCEwithLogits	28.57	1.59	30.45	12.91	30.16	20.74	69.18	62.13	50.28	75.55	77.51	81.86	44.31	67.74	76.39	76.9	65.58	40.88	48.33	77.22	66.98	65.37
	Focal	41.55	0.14	30.81	5.24	23.06	20.16	68.15	65.43	53.92	78.67	77.53	81.51	46.51	62.56	79.72	76.13	70.46	41.11	53.42	76.39	68.93	66.7
	Re-Focal	23.68	0.14	30.79	11.23	15.91	16.35	71.85	69.68	52.25	78.67	78.78	83.68	50.77	66.81	78.45	76.73	70.02	40.98	56.54	76.72	71.39	68.22
	Cross-Entropy	36.47	0.83	<b>35.42</b>	4.65	24.2	20.31	73.66	64.98	51.99	75.61	77.96	84.05	46.85	66.4	75.29	79.23	70.37	41.69	52.23	78.26	69.17	67.18
	Re-Cross-Entropy	35.59	1.3	38.54	12.54	31.71	23.93	70.71	67.85	48.91	76.36	78.06	82.38	49.33	68.88	78.77	78.7	69.41	40.87	56.92	77.58	68.21	67.53
	TCL-2	<b>44.05</b>	<b>9.09</b>	29.74	<b>30.28</b>	40.9	<b>30.81</b>	64.75	60.22	50.98	73.25	74.53	75.68	42.18	59.55	69.3	73.94	62.4	37.19	42.58	71.69	67.77	61.73
	<b>Ours</b>	43.57	3.03	26.28	8.77	34.58	23.24	74.94	65.33	53.83	73.41	77.16	80.42	46.47	62.36	74.49	77.22	68.61	42.38	56.93	78.05	69.73	66.76
5	YOLO-joint	0.0	0.0	0.0	0.0	9.1	1.8	78.0	71.5	62.9	81.7	79.7	86.8	50.0	72.3	81.7	77.9	75.6	48.4	65.4	83.2	73.6	72.6
	YOLO-ft	0.8	0.2	11.3	5.2	0.0	3.5	78.6	72.4	61.5	79.4	81.0	87.8	48.6	72.1	81.0	79.6	73.6	44.9	61.4	83.9	74.7	72.0
	YOLO-ft-full	10.3	9.1	17.4	43.5	0.0	16.0	76.4	69.6	59.1	80.3	78.5	87.8	42.1	72.1	76.6	77.1	70.7	43.1	58.0	82.4	72.6	69.8
	<b>Baseline</b>	33.1	9.4	38.4	25.4	44.0	30.1	73.2	65.6	52.9	75.9	77.5	80.0	43.7	65.0	73.8	78.4	68.9	39.2	56.4	78.0	70.8	66.6
	BCEwithLogits	34.95	9.6	39.77	38.42	35.25	31.6	62.67	60.27	47.94	73.84	76.02	81.24	36.22	58.34	70.32	76.77	64.08	34.21	44.07	67.14	68.85	61.46
	Re-BCEwithLogits	39.54	<b>10.18</b>	29.8	39.16	41.09	31.95	68.47	62.8	50.71	75.66	75.9	82.76	38.52	64.22	66.51	76.59	65.42	36.26	47.94	77.55	66.9	63.75
	Focal	36.72	9.25	38.45	19.4	33.85	27.54	71.35	63.31	50.51	78.66	77.23	82.49	43.95	60.1	76.13	77.55	70	37.36	53.92	77.12	69.18	65.92
	Re-Focal	39.04	9.27	37.96	28.32	28.4	28.6	68.26	66.08	51.29	78.9	77.25	83.35	44.7	65.53	76.78	74.94	68.89	38.34	54.3	77.37	70.51	66.43
	Cross-Entropy	37.34	9.86	34.27	38.2	39.86	31.91	70.22	59.53	47.57	74.56	75.95	82.2	43.24	65.92	68.43	76.71	68.36	35.22	50.16	77.82	67.55	64.23
	Re-Cross-Entropy	38.61	9.65	<b>42.49</b>	39.82	<b>47.31</b>	35.58	67.01	62.41	52.4	74.6	74.65	80.34	42.02	67.56	73.28	75.78	67	38.57	50.48	74.02	67.88	64.53
	TCL-2	<b>47.64</b>	9.41	36.71	41.67	39.97	35.08	64.22	60.49	52.15	75.61	73.65	78.92	36.39	58.68	70.4	75.1	62.92	32.91	45.41	75.02	67.69	61.97
	<b>Ours</b>	44.66	9.88	37.51	<b>55.49</b>	40.75	<b>37.66</b>	64.54	63.48	50.68	75.2	74.96	77.02	38.67	59.23	71.05	75.06	64.4	35.82	52.06	74.45	68.15	62.98

Table 6. The results of detection APs (%). For few-shot detection on Pascal VOC, ours significantly outperforms others on novel set3.

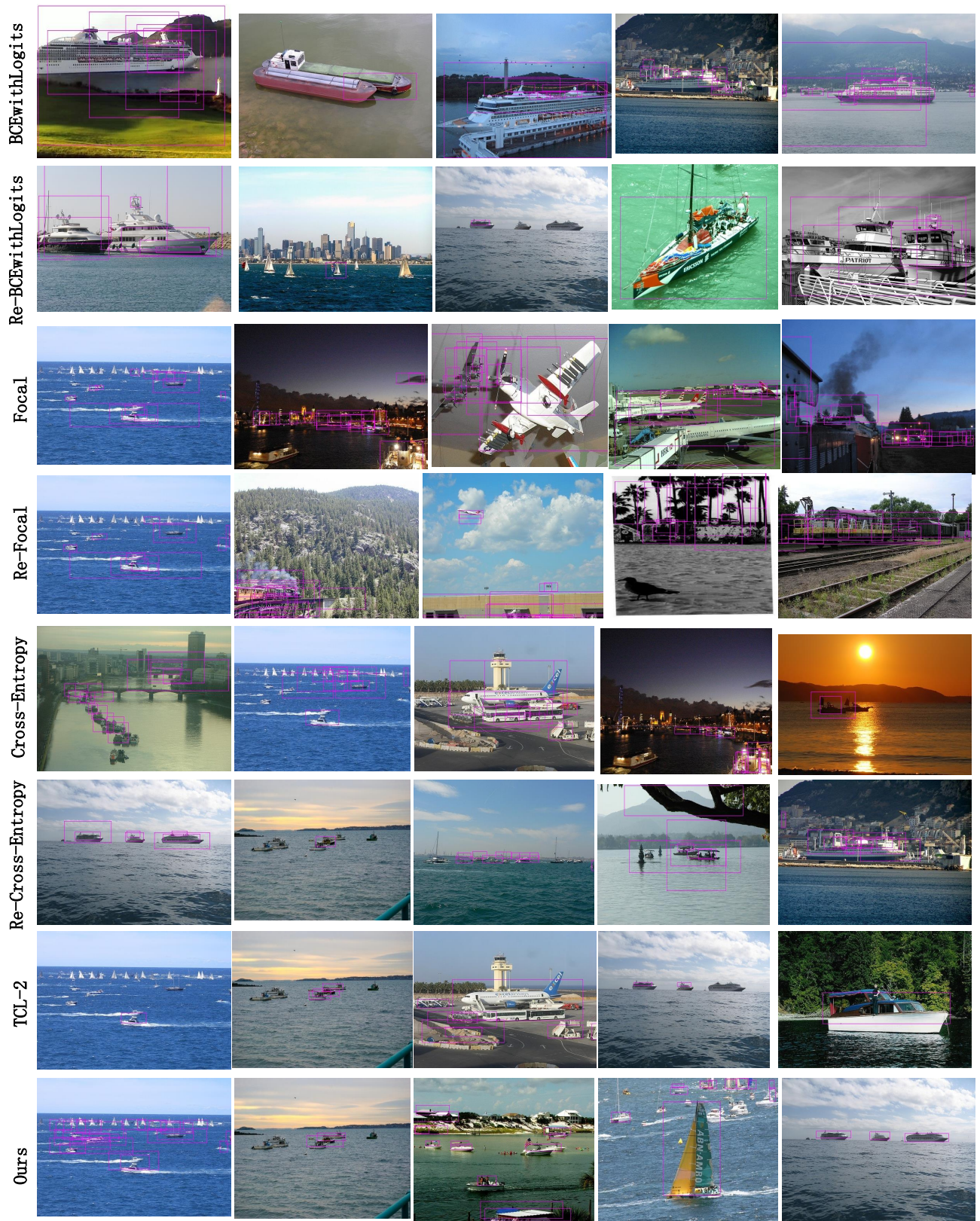


Figure 5. Qualitative 2-shot boat detection results on our test set for novel set1. We visualize the bounding boxes of all methods.



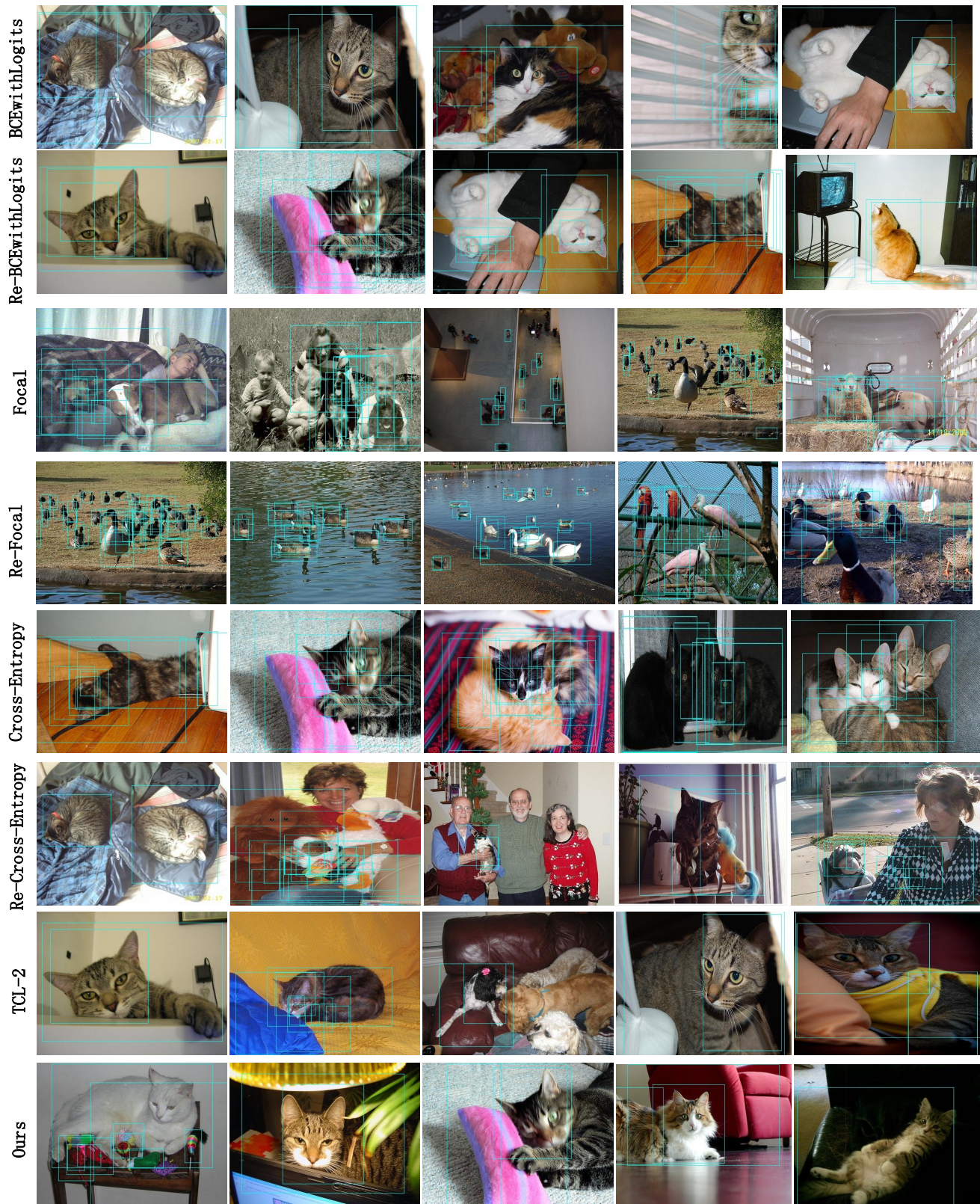
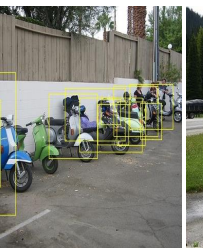
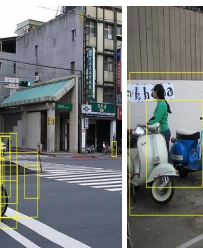


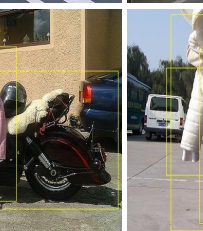
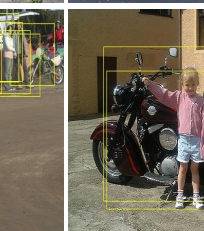
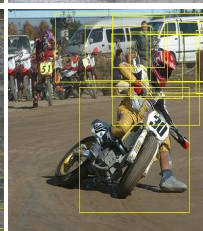
Figure 6. Qualitative 2-shot cat detection results on our test set for novel set1. We visualize the bounding boxes of all methods.



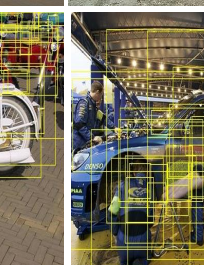
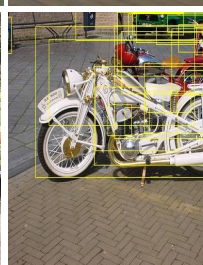
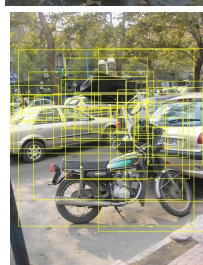
BCEwithLogits



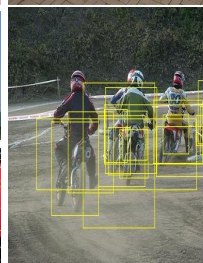
Re-BCEwithLogits



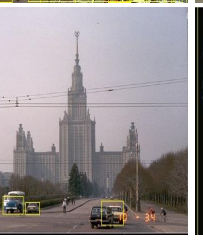
Focal



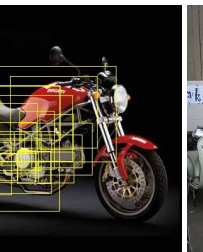
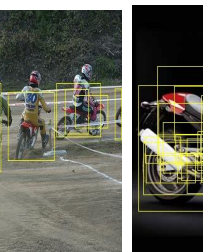
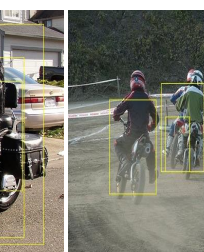
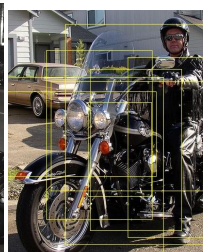
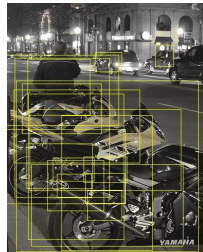
Re-Focal



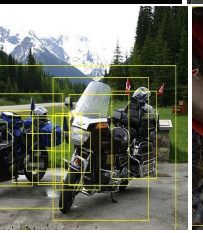
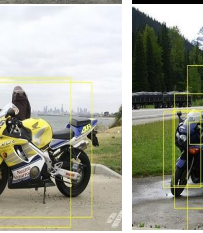
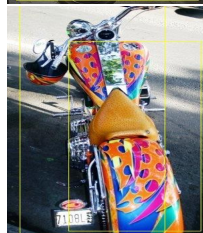
Cross-Entropy



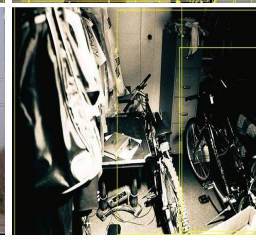
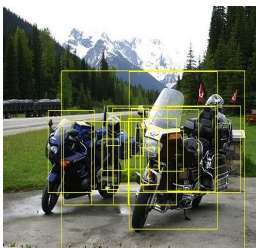
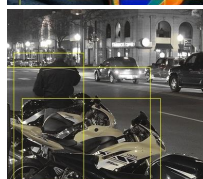
Re-Cross-Entropy



TCL-2

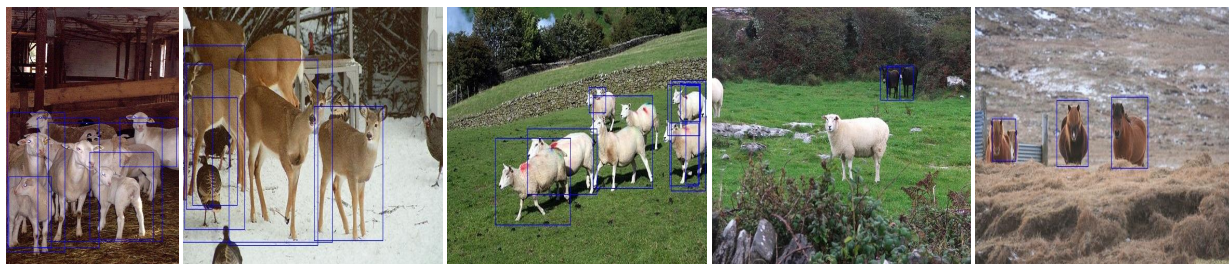


Ours

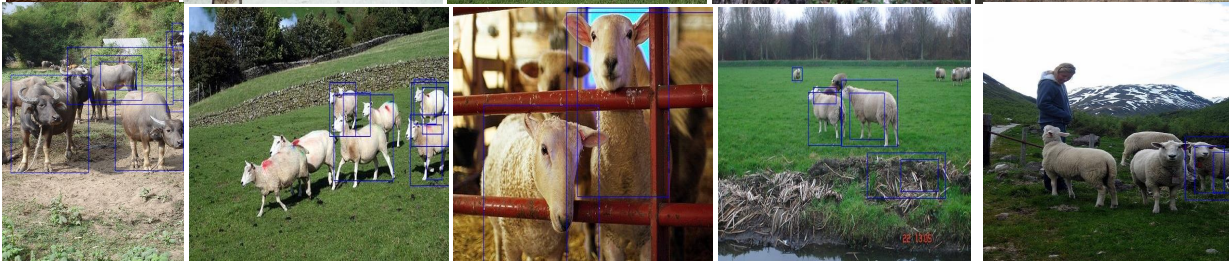




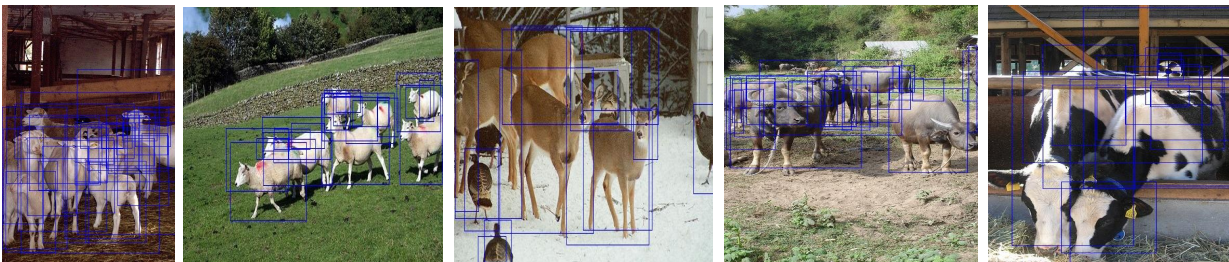
BCEwithLogits



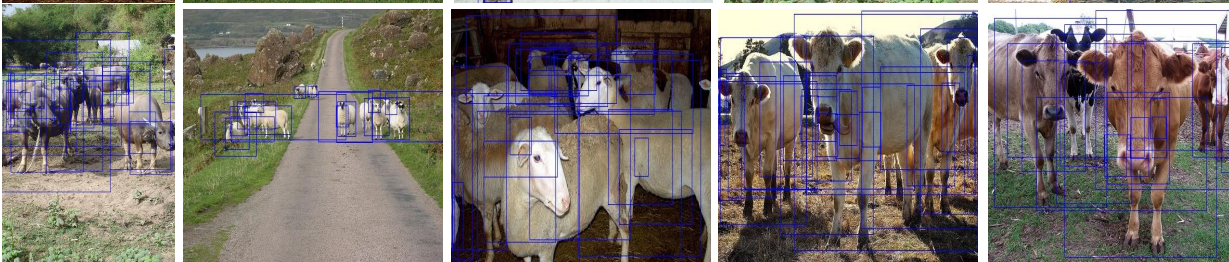
Re-BCEwithLogits



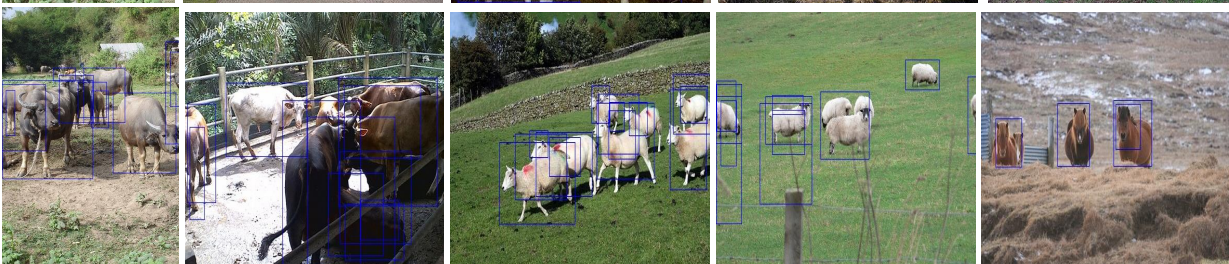
Focal



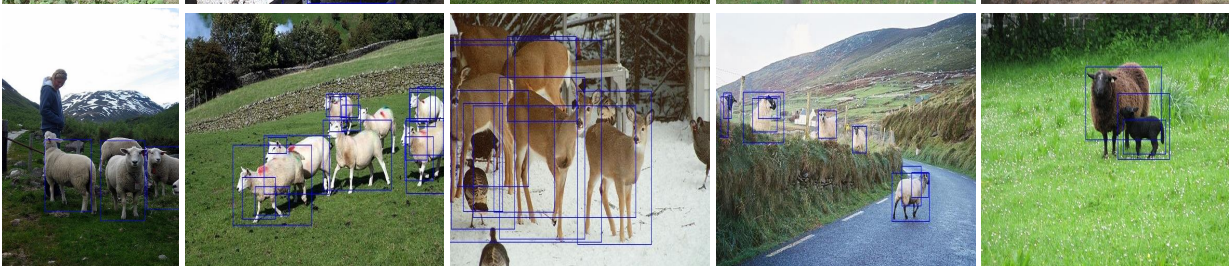
Re-Focal



Cross-Entropy



Re-Cross-Entropy



TCL-2

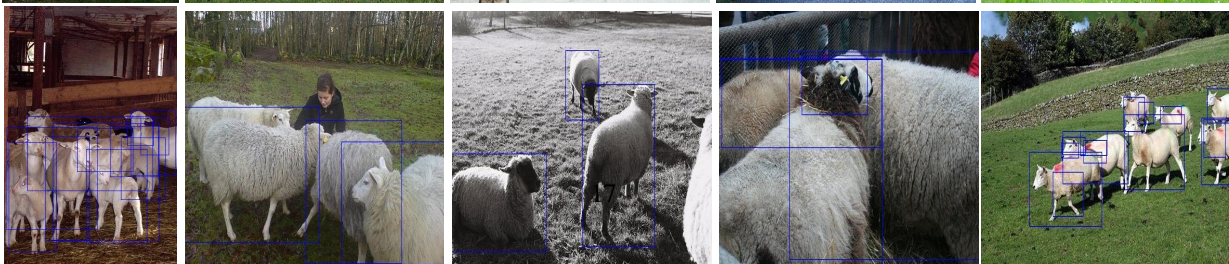






Figure 9. Qualitative 2-shot sofa detection results on our test set for novel set1. We visualize the bounding boxes of all methods.